

High Performance of Commercial Solar Cells Stacked by Crystalline p-n Silicon Nanowires

Lotfia El Nadi^{1,2#}, Mohamed Ezzat^{2,3,4} and Yehia Ismail⁵

¹Physics Dept., Laser Physics Lab., Faculty of Science, Cairo University, Giza, EGYPT

²(IC-SAS) High Density Lasers, National Institute of Laser Enhanced Sciences, Cairo Univ., Giza, EGYPT

³Laser Institute for Research and Applications LIRA, Beni-Suef University, Beni-Suef 62511, Egypt

⁴Center for Relativistic Laser Science, Institute for Basic Science (IBS), Gwangju 61005, Republic of Korea.

⁵Center of Nanoelectronics and Devices (CND), Zewail City of Science and Technology/American University in Cairo, Cairo, Egypt

Abstract: The nano-wires were prepared by Liquid Phase Pulsed Laser Ablation LP-PLA method of p-n Si wafers in distilled water. Nitrogen UV laser was used at different power with total average laser powers up to 0.539 GW/cm², to ablate p-n CZ Si crystalline wafers in double distilled water. The formed nano-wires were characterized using High Resolution Transmission Electron Microscope HRTEM and Selected Area Electron Diffraction SAED. The optical properties of the prepared nano-wires were measured to determine the highest optical absorption as a function of p-n Si crystalline sizes. The Photoluminescence spectra of the samples were also measured utilizing photo-excitation at 438.3±0.15 nm. Such optical properties suggested suitable optical properties of the nano-wires to absorb solar spectra and provide suitable and higher efficiency photons to be absorbed by the conventional solar cell thus working as antenna. Performance of the stacked device was determined by comparing the I-V characteristics of the conventional solar cells with and without the stacked p-n Si crystalline nano-wires. Higher efficiency that varied between 2.46 and 18.44% were determined.

Keywords: Si, nanowire Laser ablation; HRTEM, Abs, Solare cell.

Date of Submission: 26-03-2021

Date of acceptance: 09-04-2021

I. INTRODUCTION

The potential application for silicon has become very attractive due to the great abundance on the earth where the miniaturization led to new properties that are required in many applications such as medicine, structural materials, agricultural field the environmental bioremediation, solar cells, etc. [1-3]. Silicon nanoparticles is non-toxic for biological systems through the preparation with the appropriate structural characteristics and applied in the correct doses [4]. As silicon nanoparticle has two different types (i) silicon-nanomaterials (Si-NMs) which identical to the original silicon (Si-Si), (ii) Silica nanomaterials (silicon oxide, SiO₂), that has great thermal stability and mechanical resistance which lead to approximately the ideal substrates for functionalization in technological platform for Opto-and microelectronic circuits, antibodies [5,6], proteins, and small molecules [7,8].

The optical properties of silicon nanostructures such as; silicon nanoparticles (Si NPS) [11], porous silicon [12,13], and silicon nanowire [14], depends not only on the sizes of silicon nanocrystals but also on the chemistry of nanocrystal surface [15,16] make them very promising material for solar cell and light-emitting devices. Where various enriched oxide (SiO₂) systems have been proposed such as SiO₂ layer doped with silicon nanoparticles [17], oxidized porous silicon [18], and Si/SiO₂ superlattices [19]. for achieving high emission yield in UV-visible wavelength range.

For more than 20 years silicon solar cells are dominating the world market, but the power conversion, despite world active efforts is still around 23-25% efficiency. Ever since the establishment of solar cells, the amorphous silicon solar cells form more than 78% of the world photo-voltaic market. Multijunction technology of semiconductors was adopted to convert efficiently the solar spectrum to electric energy, known as Power Converging Efficiency (PCE). However, the Multijunction Solar Cells MJSC are expensive devices to produce [20-22]. Recently semiconductor nanowires structures attracted considerable attention [23]. Looking for materials of excellent electronic and optical properties, Silicon (Si) materials have excellent electronic and optical properties that can be obtained by fabricating nanostructures. Silicon nanowires are significant one-dimensional semiconductors and have exceptional electronic and optical properties compared to that of parent bulk Si.

The wide industry of conventional solar cells will not be affected, while the new Si wires industry [24-26] might flourish. One of the techniques for synthesis nanoparticles is the liquid phase pulsed laser ablation technique that's an effective and simple method to prepare nanoparticles from solid targets [27-30]. Where pulsed laser irradiates a material, its energy is absorbed depending on the absorption characteristics of the

material. wherein metal, the transfer of energy causes the movement of the free electrons across the surface. However, in a non-metallic material bound electrons to vibrate, which leads to an increase in the temperature of the material. these increases in the temperature can cause different phenomena on the material surface depending on the amount of energy and the duration of the incident pulse, such as fusion, vaporization and forms a plasma [31]. One of the phenomena is the ablation that is observed as the partial or total destruction of the surface. By increasing the deposited energy above the threshold of the material, the vibration and increasing the temperature produces the electrons to detach from their bonds and break the atomic structure [32,33].

Recently, this technique considers as a one-step green synthesis for efficient bio-conjugated nanoparticles which has many practical applications in fluorescence imaging and drug delivery [34-37]. High yield preparation of blue-emitting ultra-small colloidal Si NPS (1– 3 nm) by nanosecond pulse laser ablation of porous Si powder in an organic solution demonstrated by Nakamura et al., [38]. Also, the synthesis of silicon nanoparticles with a diameter range of 1–10 nm by ablating porous silicon wafer using femtosecond laser in liquid medium reported by Vendamani et.al.[39].

In this work we synthesis p-n Si nanowires by liquid-phase pulsed laser ablation. That's used to fabricate a device by stacking crystalline p-n Si nano-wires on top of conventional silicon solar cells. Where Si nanowires can absorb [40-46] the parts of the solar spectrum that are not utilized by the commercial cells and emit photons suitable to be absorbed by the commercial cells. The suitable nanowires were then used as an antenna to harvest part of the solar light and emit an extra light spectrum to be absorbed by the commercial solar cell.

II. EXPERIMENTAL DETAILS

In the present experiment, CZ monocrystalline wafers of p-n-Silicone semiconductors wafer with dimensions of $2 \times 2 \text{ cm}^2$ surface area and $2 \text{ }\mu\text{m}$ thickness. The Chemical compositions of target materials (wt%) obtained through EDX measurements are illustrated in Table 1. The wafer was carefully cleaned by alcohol spray in the air and then immersed in 3ml double distilled water placed in a quartz cell. Pulses from the PIN Nitrogen UV laser were employed in the ablation of the silicon wafer immersed in the double-distilled water as illustrated in figure 1. The 0.2 HZ Nitrogen laser provided laser pulses of $\lambda = 337 \text{ nm}$ wavelength, pulse duration of 15 nanoseconds, and power 337mJ/ pulse. Several samples were prepared using a different number of pulses starting from 50 pulses up to 800 pulses. The transparent solution of each sample was introduced into an ultrasonic vibration system for 30 minutes until they turned greyish in color forming the colloidal solution of nanocrystal silicon wires.

Table 1: Chemical compositions of target materials (wt%).

Element	Weight%	Atomic%
O K	6.12	10.30
Si K	92.62	88.85
Ca K	1.26	0.85

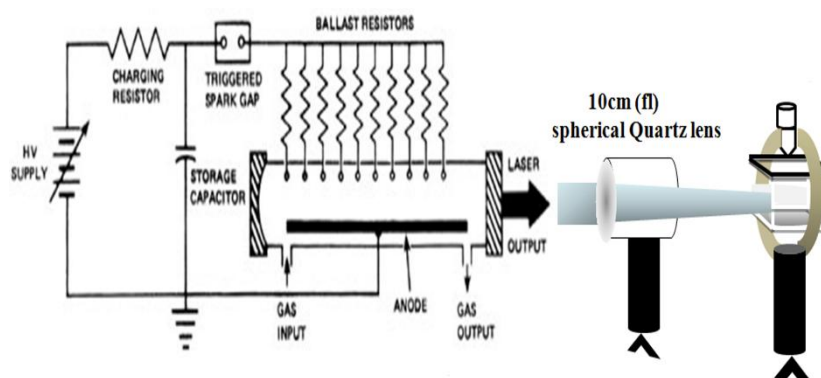


Fig.1 Schematic representation of the experimental set up: the Nitrogen laser system is represented on the left hand side and the UV emerging Laser beam was focused by a spherical quartz lens on the surface area of clean p-n-Si sheet immersed in double distilled water, in a quartz cell as shown on the right hand side of the figure.

The different samples were characterized each at a time by HRTEM High-Resolution Transmission Electron Microscope (HRTEM JEOL JEM-2100) and Selected Area Electron Diffraction ED measurements.

Optical absorption spectra in the range of 200 to 900 nm were measured for each sample using UV-Visible spectrophotometer type (UV-Vis PG Ins. Ltd T80+). Photoluminescence measurements were measured using the system shown in figure 2, where Argon laser providing laser wavelength $490 \pm 1.21\text{nm}$ of power output approximately 50 mW, was used.

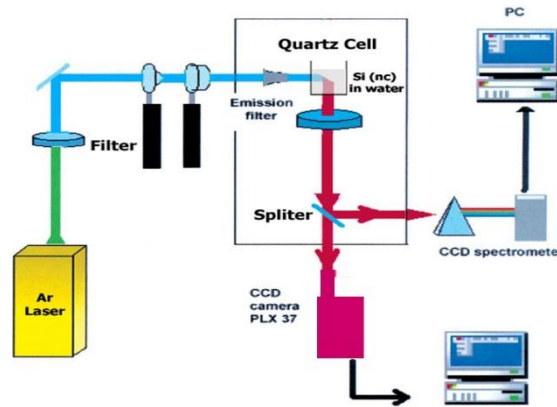


Fig. 2 Photoluminescence measurement System

III. RESULTS AND DISCUSSION

HRTEM images were performed to study the effect of the laser shots on synthesis of silicon nanoparticles in doubled distilled water as shown in figures 3(a–d). By beginning Ablating the p-n Si wafers in distilled water with total average laser power of 3.37W (50 shots) silicon nano-wires start to form although it wasn't sufficient enough as illustrated in figure 3(a) showed with average length 114.035 nm and average diameter $\sim 15.52 \pm 1.15\text{nm}$. We systematically increased the laser shots until we reached 800 pulses making sure to keep the same conditions of the laser pulses and specially the energy per pulse. Ablating the p-n Si wafers in distilled water by depositing total average laser power of 6.74W (100 laser pulses) the crystalline nanowires formed with average length 71.982 nm and average diameter $\sim 12.03 \pm 0.35\text{nm}$ as seen in figure 3(b) and nanowire density $\sim \times 10^{10}/\text{cm}^2$.

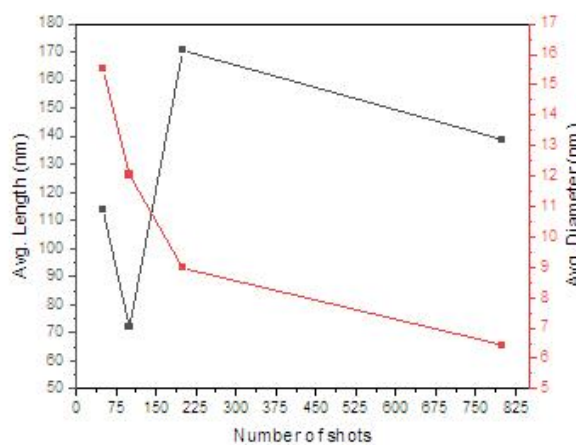
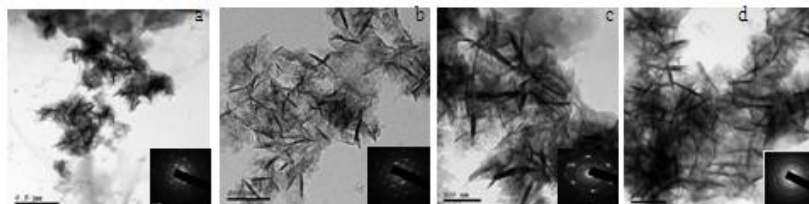


Fig. 3 HRTEM and ED images for the p-n Silicon nano-wires at (a)50,(b)100,(c)200 and (d)800 Laser pulses. (e) show the relation between the average length and the average diameter with the laser shots.

While increasing the total average laser power to be 13.48W (200 laser pulses) deposited in p-n Si wafers in distilled water the Si nanowires synthesis with average length 170.579 nm and average diameter of

$\sim 8.97 \pm 0.15 \text{ nm}$ and nanowire density of $\sim \times 10^{12} / \text{cm}^2$, figure 3(c). By depositing the total average laser power of 53.92W (800 laser pulses) in p-n Si wafers in distilled water we obtained Si nanowires with average length 138.808 nm and average diameter $\sim 6.444 \pm 2.75 \text{ nm}$ and nanowire density of $\sim \times 10^{13} / \text{cm}^2$ as illustrated in figure 3(d).

The nano-wires selected area electron diffraction of each sample shown inset of the figures indicates (111) p-n Si Crystalline structure as in the originally used wafers irrespective of the applied ablating conditions. Most important is the clarity of the diffraction rings and high clarity which might be attributed to the density of the p-n Si nano-wires.

Figure 3(e) show the relation between the number of laser shots with the average length and average diameter as illustrated the average diameter decrease gradually by increasing the number of shots while the particles density increase.

The optical absorption spectra of the different p-n Si crystalline nanowires formed by LP-LPA using different laser shots (50, 100, 200 and 800) of the UV nitrogen laser are given in figure 4(a). One notices that the optical absorption of the different n-p Si nanowires for optical spectrum ranging from 200 nm to 450 nm (important-range of the solar UV spectrum) shows interesting features.

The optical absorption spectrum-for all the samples show nearly constant absorption value for the photons of wavelength range from 0.460 μm to 0.720 μm comprising the UV of the solar spectrum. The absorption coefficient of the 0.220 μm photons varies slowly from 0.55 to 0.65 ABS (norm) for the samples prepared by 50 to 200 UV laser Shots. While it shoots up to 0.85 ABS (norm) for the samples prepared by 800 shots. A small peak shown at wavelength 0.750 μm for samples ablated at 100,200 and 800 laser shots. At photons of wavelength 0.940 μm the absorption drops for all the samples to 0.13, 0.44 ABS (norm) for the first three samples. While it drops to 0.64 ABS (norm) for samples prepared by 800 UV laser shots.

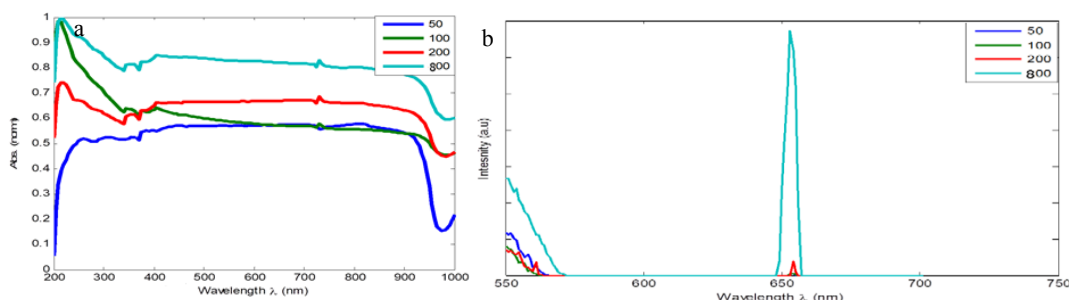


Fig. 4 (a) shows the absorption Spectra for p-n Si nanowires. (b) The photoluminescence spectra for all the crystalline p-n Si nanowires formed by 50, 100,200 and 800 UV laser shots

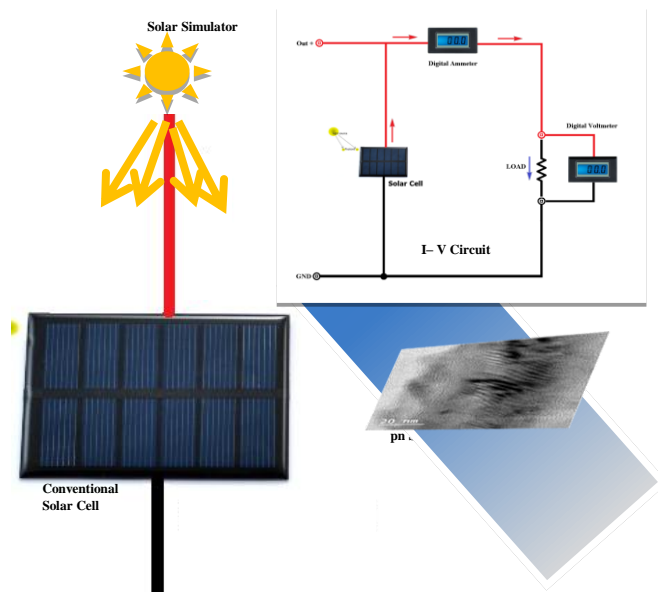
The photoluminescence spectra given in figure 4(b) for all the samples exhibit the same photoluminescence line centered at $615 \pm 0.15 \text{ nm}$. For the sample prepared by 800 UV laser shots, relatively high PL spectral intensity is encountered. This is in accordance with previous inherent absorption spectra.

The I-V characteristic were carried out after treating the samples by ultrasonic shaker. Equal number of drops from each sample taken by fine needle were placed between two glass covers of a microscope and placed on the commercial solar cell with illuminating solar simulator. The measurements were taken for the commercial cell with and without the samples and using a solar simulator, schematic diagram shown in figure 5(a).

As illustrated in figure 5(b) the I-V value enhance gradually with laser shots which relative to the diameter of the nanowire and the particles density, where largest value achieved during using 800 shots for ablated p-n Si. The nanowires fluoresce in the visible range. This means the increase of the light intensity suitable to be absorbed by the commercial cells.

One can say that the p-n Si nanowires are fluorophores. We conclude that:

- 1) Nanowires prepared by 50 UV laser shots produced 2.46% efficiency increase
- 2) Nanowires prepared by 100 UV laser shots produced 10.82% efficiency increase
- 3) Nanowires prepared by 200 UV laser shots produced 16.804% efficiency Increase
- 4) Nanowires prepared by 800 UV laser shots produced 18.446% efficiency Increase.



I want to correct (b) by $\times 1/2$ for the y axis without nanowires

a

Fig.5. (a) schematic diagram for the I-V circuit, (b) measurements of I-V with and without silicon nanowires

IV. CONCLUSION

In this study the commercial solar cells were used as manufactured, no change of the conventional solar cells structure was approached. The p-n Si nanowires were utilized as an extra source of light or as fluorescent material that absorbs the solar UV spectral intensity, which is not utilized by the commercial solar cells. The nanowires fluoresce in the visible range, which indicates the increase in the light intensity suitable to be absorbed by

the commercial cells. One might call them antennas to collect the UV part of the solar radiation.

ACKNOWLEDGMENT

The authors would like to acknowledge the assistance of the Laser Physics Lab. team at the Faculty of Science, Cairo University for permitting the use of the UV Nitrogen Laser. Many thanks are due to the International Arab Optronics Company for providing the p-n Silicon wafers.

Conflicts of Interest:

The authors declare no conflicts of interest.

Author Contributions

These authors contributed equally: Lotfia El Nadi and Mohamed Ezzat

REFERENCES

- [1]. Jeelani, P.G.; Mulay, P.; Venkat, R.; Ramalingam, C. Multifaceted Application of Silica Nanoparticles. A Review. *Silicon* 2020, 12, 1337–1354. [CrossRef]
- [2]. Nayfeh, M.H.; Mitas, L. Chapter One-Silicon Nanoparticles: New Photonic and Electronic Material at the Transition between Solid and Molecule; Kumar, V.B.T.-N., Ed.; Elsevier: Amsterdam, The Netherlands, 2008; pp. 1–78. ISBN 978-0-08-044528-1.
- [3]. Gribov, B.G.; Zinov'ev, K.V.; Kalashnik, O.N.; Gerasimenko, N.N.; Smirnov, D.I.; Sukhanov, V.N.; Kononov, N.N.; Dorofeev, S. G. Production of Silicon Nanoparticles for Use in Solar Cells. *Semiconductors* 2017, 51, 1675–1680. [CrossRef]
- [4]. Jaganathan, H.; Godin, B. Biocompatibility assessment of Si-based nano- and micro-particles. *Adv. Drug Deliv. Rev.* 2012, 64, 1800–1819.
- [5]. Bouchoucha, M.; Béliveau, É.; Kleitz, F.; Calon, F.; Fortin, M.-A. Antibody-conjugated mesoporous silica nanoparticles for brain microvessel endothelial cell targeting. *J. Mater. Chem. B* 2017, 5, 7721–7735. [CrossRef]
- [6]. McInnes, S.J.P.; Turner, C.T.; Al-Bataineh, S.A.; Airaghi Leccardi, M.J.I.; Irani, Y.; Williams, K.A.; Cowin, A.J.; Voelcker, N.H. Surface engineering of porous silicon to optimise therapeutic antibody loading and release. *J. Mater. Chem. B* 2015, 3, 4123–4133. [CrossRef] [PubMed]
- [7]. Sheykhzadeh, S.; Luo, M.; Peng, B.; White, J.; Abdalla, Y.; Tang, T.; Mäkilä, E.; Voelcker, N.H.; Tong, W.Y. Transferrin-targeted porous silicon nanoparticles reduce glioblastoma cell migration across tight extracellular space. *Sci. Rep.* 2020, 10, 2320. [CrossRef]
- [8]. Martinez-Carmona, M.; Baeza, A.; Rodriguez-Milla, M.A.; Garcia-Castro, J.; Vallet-Regí, M. Mesoporous silica nanoparticles grafted with a light-responsive protein shell for highly cytotoxic antitumoral therapy. *J. Mater. Chem. B* 2015, 3, 5746–5752. [CrossRef] [PubMed]
- [9]. López, V.; Villegas, M.R.; Rodríguez, V.; Villaverde, G.; Lozano, D.; Baeza, A.; Vallet-Regí, M. Janus Mesoporous Silica Nanoparticles for Dual Targeting of Tumor Cells and Mitochondria. *ACS Appl. Mater. Interfaces* 2017, 9, 26697–26706. [CrossRef]
- [10]. Jafari, S.; Derakhshankhah, H.; Alaei, L.; Fattahi, A.; Varnamkhasti, B.S.; Saboury, A.A. Mesoporous silica nanoparticles for therapeutic/diagnostic applications. *Biomed. Pharmacother.* 2019, 109, 1100–1111. [CrossRef]
- [11]. Kanemitsu Y (1994) Luminescence properties of nanometer-sized Si crystallites: Core and surface states. *Phys Rev B* 49:16845–16848
- [12]. Tsybeskov L, Vandyshev JV, Fauchet PM (1994) Blue emission in porous silicon: Oxygen-related photoluminescence. *Phys Rev B* 49: 7821–7824
- [13]. Kontkiewicz AJ, Kontkiewicz AM, Siejka J, Sen S, Nowak G, Hoff AM, Sakhivel P, Ahmed K, Mukherjee P, Witanachchi S (1994) Evidence that blue luminescence of oxidized porous silicon originates from SiO₂. *Appl Phys Lett* 65:1436–1438
- [14]. Lee M, Peng K (1993) Blue emission of porous silicon. *Appl Phys Lett* 62:3159–3160
- [15]. Zhu M, Chen G, Chen P (1997) Green/blue light emission and chemical feature of nanocrystalline silicon embedded in siliconoxide

- thin film. *Appl Phys A Mater Sci Process* 65:195–198
- [16]. Qin G, Song H, Zhang B, Lin J, Duan J, Yao G (1996) Experimental evidence for luminescence from silicon oxide layers in oxidized porous silicon. *Phys Rev B* 54:2548–2555
- [17]. Pavese L, Dal Negro L, Mazzoleni C, Franzo G, Priolo F (2000) Optical gain in silicon nanocrystals. *Nature* 408:440–444
- [18]. Kontkiewicz AJ, Kontkiewicz AM, Siejka J, Sen S, Nowak G, Hoff AM, Sakthivel P, Ahmed K, Mukherjee P, Witanachchi S (1994) Evidence that blue luminescence of oxidized porous silicon originates from SiO₂. *Appl Phys Lett* 65:1436–1438
- [19]. Averboukh B, Huber R, Cheah K, Shen Y, Qin G, Ma Z, Zong W (2002) Luminescence studies of a Si/SiO₂ superlattice. *J Appl Phys* 92:3564–3568
- [20]. Green, M. A. et al. Solar cell efficiency tables (Version 53). Beauchamp, P. M. & Cutts J. A. Solar Power Technologies for Future Planetary Science Missions. Pasadena, California: National Aeronautics & Space Administration (NASA), Jet Propulsion Lab. *Photovolt : Res. Appl.* 27, 3–12 (2019)
- [21]. Nozik, A. J., Conibeer, G. & Beard, M. C. (Eds.). *Advanced concepts in photovoltaics* (Royal Society of Chemistry, 2014).
- [22]. Garland, J. W., Biegala, T., Carmody, M., Gilmore, C. & Sivanathan, S. Next-generation multijunction solar cells: The promise of II-VI materials. *Jour. of Appl.Phys.* 109, 102423 (2011).
- [23]. Cariou, R. et al. III-V-on-silicon solar cells reaching 33% photoconversion efficiency in two-terminal configuration. *Nature Energy* 3, 326–333 (2018).
- [24]. Yang P, Zeng X, Xie X, Zhang X, Li H, Wang Z. Improved open-circuit voltage of silicon nanowires solar cells by surface passivation. *RSC Adv* 2013; 3:24971.
- [25]. Khan F, Baek SH, Kim JH. Novel approach for fabrication of buried contact silicon nanowire solar cells with improved performance. *Sol Energy* 2016; 137: 122e8.
- [26]. Wang X et al Radial junction silicon nanowire photovoltaics with heterojunction with intrinsic thin layer (HIT) structure. *IEEE J Photovoltaics* 2016, 6.
- [27]. Svrcek V, Mariotti D, Kondo M (2009) Ambient-stable blue luminescent silicon nanocrystals prepared by nanosecond-pulsed laser ablation in water. *Opt Express* 17:520–527
- [28]. Kruusing A (2010) *Handbook of liquids-assisted laser processing*. Elsevier, Amsterdam
- [29]. Dolgaev S, Simakina A, Voronov V, Shafeev G, Bozon-Verduraz F (2002) Nanoparticles produced by laser ablation of solids in liquid environment. *Appl Surf Sci* 186:546–551
- [30]. Khashan KS, Ismail RA, Mahdi RO (2018) Synthesis of SiC nanoparticles by SHG 532 nm Nd:YAG laser ablation of silicon in ethanol. *Applied Physics A* 124:443
- [31]. Kannatey-Asibu, E. Background on Laser Processing. In *Principles of Laser Materials Processing*; John Wiley & Sons, Ltd.: Hoboken, NJ, USA, 2008; pp. 407–430, ISBN 9780470459300.
- [32]. Steen, W.M. Laser material processing—An overview. *J. Opt. A Pure Appl. Opt.* 2003, 5, S3–S7. [CrossRef]
- [33]. Eason, R. (Ed.) *Pulsed Laser Deposition of Thin Films: Applications-Led Growth of Functional Materials*; John Wiley & Sons, Ltd.: Hoboken, NJ, USA, 2007; ISBN 9780470052129
- [34]. Bagga K, Barchanski A, Intartaglia R, Dante S, Marotta R, Diaspro A, Sajti C, Brandi F (2013) Laser-assisted synthesis of Staphylococcus aureus protein-capped silicon quantum dots as bio-functional nanoprobes. *Laser Phys Lett* 10:065603–065608
- [35]. Intartaglia R, Barchanski A, Bagga K, Genovese A, Das G, Wagener P, Di Fabrizio E, Diaspro A, Brandi F, Barcikowski S (2012) Bioconjugated silicon quantum dots from one-step green synthesis. *Nanoscale* 4:1271–1274
- [36]. Intartaglia R, Bagga K, Scotto M, Diaspro A, Brandi F (2012) Luminescent silicon nanoparticles prepared by ultra short pulsed laser ablation in liquid for imaging applications. *Opt Mater Express* 2:510–518
- [37]. Intartaglia R, Bagga K, Genovese A, Athanassiou A, Cingolani R, Diaspro A, Brandi F (2012) Influence of organic solvent on optical and structural properties of ultra-small silicon dots synthesized by UV laser ablation in liquid. *Phys Chem Chem Phys* 14:15406–15411
- [38]. Nakamura T, Yuan Z, Adachi S (2014) High-yield preparation of blue-emitting colloidal Si nanocrystals by selective laser ablation of porous silicon in liquid. *Nanotechnology* 25:275602–275608
- [39]. Vendamani V, Hamad S, Saikiran V, Pathak A, Rao SV, Kumar VRK, Rao SN (2015) Synthesis of ultra-small silicon nanoparticles by femtosecond laser ablation of porous silicon. *J Mater Sci* 50: 1666–1672
- [40]. Essig, S. et al. Raising the one-sun conversion efficiency of III-V/Si solar cells to 32.8% for two junctions and 35.9% for three junctions. *Nature. Energy* 2, 17144 (2017).
- [41]. Hörantner, M. T. et al. The Potential of Multijunction Perovskite Solar Cells. *ACS En.Lett.* 2, 2506–2513 (2017).
- [42]. Feifel, M.; Lackner, D.; Ohlmann, J.; Benick, J.; Hermle, M.; Dimroth, F. Direct Growth of GaInP/GaAs/Si Triple-Junction Solar Cell with 22.3% AM1.5g Efficiency. *Sol. RRL* 2019, 3, 1900313.
- [43]. Walker, A. W. et al. Impact of photon recycling and luminescence coupling on III-V single and dual junction photovoltaic devices. *Jour. of Phot. for En.* 5, 053087 (2015).
- [44]. Lan, D. & Green, M. A. Photoluminescent and electroluminescent couplings in monolithic tandem solar cells. *Prog. Photovolt.: Res. Appl.* 24, 1566–1576 (2016).
- [45]. Jevasuwan W, Pradel KC, Subramani T, Chen J, Takei T, Nakajima K, et al. Diffused back surface field formation in combination with two-step H₂ annealing for improvement of silicon nanowire-based solar cell efficiency. *Jpn J Appl Phys* 2017;56.
- [46]. Hamidinezhad H, Ashkarraan AA. Forest of ultra thin silicon nanowires: realization of temperature and catalyst size. *J Mater Sci Mater Electron* 2018; 29:5373e9.